Neurophotonics

Neurophotonics.SPIEDigitalLibrary.org

Characterization of the BAC Id3-enhanced green fluorescent protein transgenic mouse line for *in vivo* imaging of astrocytes

Cassandra Lamantia
Marie-Eve Tremblay
Ania Majewska

SPIE.

Characterization of the BAC Id3-enhanced green fluorescent protein transgenic mouse line for *in vivo* imaging of astrocytes

Cassandra Lamantia, Marie-Eve Tremblay,[†] and Ania Majewska[*]
University of Rochester, Department of Neurobiology and Anatomy, Rochester, New York 14642, United States

Abstract. Astrocytes are highly ramified glial cells with critical roles in brain physiology and pathology. Recently, breakthroughs in imaging technology have expanded our understanding of astrocyte function *in vivo*. The *in vivo* study of astrocytic dynamics, however, is limited by the tools available to label astrocytes and their processes. Here, we characterize the bacterial artificial chromosome transgenic Id3-EGFP knock-in mouse to establish its usefulness for *in vivo* imaging of astrocyte processes. Using fixed brain sections, we observed enhanced green fluorescent protein expression in astrocytes and blood vessel walls throughout the brain, although the extent and cell type specificity of expression depended on the brain area and developmental age. Using *in vivo* two-photon imaging, we visualized astrocytes in cortical layers 1–3 in both thin skull and window preparations. In adult animals, astrocytic cell bodies and fine processes could be followed over many hours. Our results suggest that Id3 mice could be used for *in vivo* imaging of astrocytes and blood vessels in development and adulthood.
 [DOI: 10.1117/1.NPh.1.1.011014]

Keywords: astrocyte; two-photon microscopy; Id3; bacterial artificial chromosome; neurodevelopment.

Paper 14042SSR received Mar. 24, 2014; revised manuscript received Aug. 6, 2014; accepted for publication Sep. 3, 2014; published online Sep. 12, 2014.

1 Introduction

Astrocytes are macroglial cells with a complex ramified morphology. These cells maintain distinct, nonoverlapping domains in the brain where they play critical homeostatic roles within brain circuits.[1] Astrocytes physically interact with blood vessels where they modulate blood flow and the blood-brain barrier,[2,3] and with synapses where their actions have profound effects on synaptic transmission and plasticity.[4] Additionally, astrocytes appear to play critical roles in neuronal development through their actions on synaptogenesis and synaptic pruning.[5,6] Recent developments in *in vivo* imaging technologies have significantly advanced our understanding of the extensive roles these cells play in neurophysiology and neuropathology.[7] *In vivo* two-photon imaging of astrocytic calcium signals has shown that astrocytes are critical elements of neural processing circuits[8–11] and that their responses to pathological stimuli are dynamic and can modulate disease progression in the central nervous system.[12–14] However, because many functions that astrocytes play are localized to their extensive arbor of very small processes that interact with capillaries and synapses, it is critically important to image the structural dynamics and function of fine astrocytic processes. Studies in brain slices have suggested that astrocytic fine processes are highly motile[15–17] and that this motility may be critical to their functions. To date, existing imaging studies have been mostly limited to examining the morphology of astrocytes and their reaction to pathological events *in vivo* due to the lack of appropriate labels that could allow the visualization of the very small processes as required to study their interactions with blood vessels and other cellular elements in the intact healthy brain.[18]

Id3 is a member of the inhibitor of DNA binding (Id) proteins which bind to and inhibit basic helix-loop-helix transcription factors. Id proteins are expressed largely during embryonic development, but have also been shown to be present in the postnatal brain.[19] Recently, GENSAT created a bacterial artificial chromosome (BAC) transgenic Id3 mouse, where enhanced green fluorescent protein (EGFP) can be used to track Id3 expression in the murine brain (Tg(Id3-EGFP)FS137Gsat).[20] Here, we use this mouse to characterize Id3 expression in the postnatal mouse brain and to establish the usefulness of this mouse strain for *in vivo* imaging purposes at different ages. We find that Id3 is expressed in astrocytes and blood vessel walls across cortical areas and layers between postnatal day (P) 7 and P61 *in situ*. While many blood vessels are labeled with EGFP in these mice, expression in astrocytes is patchy which allows for *in vivo* imaging of fine astrocytic processes. *In vivo* two-photon imaging was also able to resolve fine astrocytic structures in the adult cerebral cortex. We conclude that the BAC Id3 transgenic mouse can be used for *in vivo* imaging of fine astrocytic structures throughout postnatal life.

2 Materials and Methods

2.1 *Animals*

Tg(Id3-EGFP)FS137 Gsat mice were obtained from Mutant Mouse Regional Resource Centers (MMRRC) University of California, Davis.[20] Mice of different ages, including early postnatal development—P7; adolescence—P28; and early adulthood—P61, were used to characterize the expression of

*Address all correspondence to: Ania Majewska, E-mail: Ania_Majewska@urmc.rochester.edu

†Present address: Université Laval, Faculty of Medicine, CHU de Québec Research Center, Department of Molecular Medicine, Québec G1V 4G2, Canada.

0091-3286/2014/$25.00 © 2014 SPIE

EGFP. GLT-1 eGFP BAC promoter reporter mice[21] were used as adults (>P90). The animal and experimental protocols were approved by the University of Rochester University Committee on Animal Resources (UCAR) in accordance with the Public Health Service (PHS) policy on humane care and use of laboratory animals and conformed to the National Institute of Health Guidelines.

2.2 *Immunohistochemistry*

Mice were deeply anesthetized with sodium pentobarbital (80 mg/kg, i.p.) and perfused transcardially with 100-mM phosphate buffered saline (PBS) and then with 4% paraformaldehyde (PFA) in 100-mM phosphate buffer. After postfixation in 4% PFA at 4°C, the brains were cryoprotected in 10%, 20%, and 30% sucrose and flash frozen. The brains were coronally sectioned at 50 μm on a freezing microtome (HM 430 Microtome; MICROM International GmbH, Walldorf, Germany). The tissue was cut into cryoprotectant and frozen at −20°C. For immunofluorescence staining, the tissue was removed from the cryprotectant and washed three times for 15 min each in 0.1 M PBS. For analysis of EGFP expression, six animals per age group and three sections of tissue per area were analyzed. For immunohistological analysis, sections were placed in a solution containing 3% H_2O_2 and 0.1 M PBS for 20 min. Sections were washed three times for 15 min in 0.1 M PBS. Sections were then blocked for 1 h in a solution containing 5% normal donkey serum, and 0.3% Triton-X-100 in 0.1 M PBS. Sections were then washed again in 0.1 M PBS and placed in the primary antibodies: rabbit anti-Iba1, (1:500, Wako Chemicals USA, Inc., Richmond, Virginia), mouse anti-neuronal nuclei (NeuN, 1:500, Millipore, Billerica, Massachusetts), rabbit anti-glial fibrillary acidic protein (GFAP, 1:2000, DAKO), rabbit anti-GFP (1:3000, Invitrogen, Grand Island, New York) at 4°C, shaking for 48 h. Sections were washed and incubated in secondary antibodies (AlexaFluor 594 Donkey anti-rabbit IgG, 1:250; AlexaFluor 594 Donkey anti-mouse IgG, 1:250; AlexaFluor 594 Donkey anti-mouse IgG, 1:250; Alexa 594 Donkey anti-rabbit 1:500, Molecular Probes, Carlsbad, California) for 4 h. Sections were rinsed in 0.1 M PBS, mounted on slides, and coverslipped with ProLong Gold anti-fade (Molecular Probes, Carlsbad, California) then edges were sealed and slides were protected from light until analysis.

2.3 *Image Acquisition and Analysis*

The mouse brain atlas was used to locate brain areas to be analyzed.[22] For analysis of EGFP expression, images were taken using epifluorescence on a Olympus BX51 epifluorescence microscope (Olympus, Center Valley, Pennsylvania) using a 10×0.3 NA objective and a 20×0.5 NA objective (Olympus). Digital images were acquired with a Spot Insight Color camera (Diagnostic Instruments, Sterling Heights, Michigan) and Image Pro software (Media Cybernetics, Bethesda, Maryland), and acquisition parameters were kept constant for imaging of all sections. An observer blinded to age analyzed the expression of EGFP in astrocytes and blood vessels with a scoring system where 0 corresponded to no staining and 3 corresponded to intense staining. Scores from all animals were averaged and rounded to the nearest number. The density of labeled structures was scored with the same system. Lastly, the appearance of astrocytes was scored as N (for net—many astrocytes grouped together) and S (single—individual astrocytes are labeled with clear visualization of the process arbor). For observation of co-localization of EGFP with different immunohistological markers, images were collected on a Zeiss LSM 500 confocal microscope (Thornwood, New York) using a 40×1.2 NA lens and a 100×1.46 NA lens (Zeiss). Co-localization was observed qualitatively and no quantification was attempted.

2.4 *In Vivo Two-Photon Imaging*

For two-photon imaging, mice were anesthetized with avertin (16 μg/g of body weight; i.p.); the skull was exposed and cleaned of membranes. The skull was then dried and glued to a thin metal plate using Loctite 454 gel glue (Prism, Rocky Hill, Connecticut). The glue was dried using an accelerator (Zipkicker, Pacer Technology, Rancho Cucamonga, California), which was pipetted onto the skull. Care was taken not to allow the accelerator to touch the mouse's eyes. Primary visual cortex (V1) was identified according to stereological coordinates. The skull above the imaged area was thinned with a dental drill or a small craniotomy was made and sealed with agarose and a coverslip.[23] The procedure was frequently interrupted to apply cold saline to the skull in order to prevent brain injury and astrocytic activation. During surgery and imaging, the animal's temperature was kept constant with a heating pad and the anesthesia was maintained with periodic administration of avertin. A custom-made two-photon scanning microscope[24] was employed, using a wavelength of 920 nm and a 20×0.95 NA objective lens (Olympus, Melville, New York) at 10× digital zoom. Images were acquired as z stacks with a 1–5-μm step size. Time-lapse images were acquired as z-stacks every 5 min.

3 Results

To determine whether BAC Id3 EGFP mice could be useful for *in vivo* imaging of astrocytic structure, we first examined EGFP fluorescence in fixed brain sections from these mice. Blood vessels were clearly delineated by EGFP fluorescence and occasional astrocytes were also visible [Figs. 1(a) and 1(b)]. Astrocytic cell bodies and detailed morphology of astrocytic processes could easily be seen in the labeled astrocytes in adult animals [P61; Fig. 1(c)]. To determine how well the astrocytic morphology could be delineated based on EGFP expression alone, we immunostained sections from BAC Id3 eGFP mice with an anti-GFP antibody. While anti-GFP staining provided a sharper image of fine processes, most of the astrocytic arbor, including distant processes, was well visualized by EGFP fluorescence alone and a high degree of co-localization between anti-GFP staining and EGFP fluorescence was observed throughout the astrocyte (Fig. 2). This suggests that expression of EGFP is high even in small, distant areas of the astrocytic arbor and that these areas can be visualized without signal amplification.

To determine the developmental expression of EGFP in these mice, we examined fixed brain sections at different ages (P7, P28, and p61; $n = 6$ animals each) in different brain areas (Fig. 3). EGFP appeared restricted to astrocytes and blood vessel walls at all ages. We observed staining in all parts of the brain, although the extent of EGFP expression and the cell types labeled depended on brain area and developmental age. To get a more thorough picture of the effect of developmental age on EGFP expression, an observer, blinded to age, categorized expression in astrocytes and blood vessels in different brain areas (Table 1).

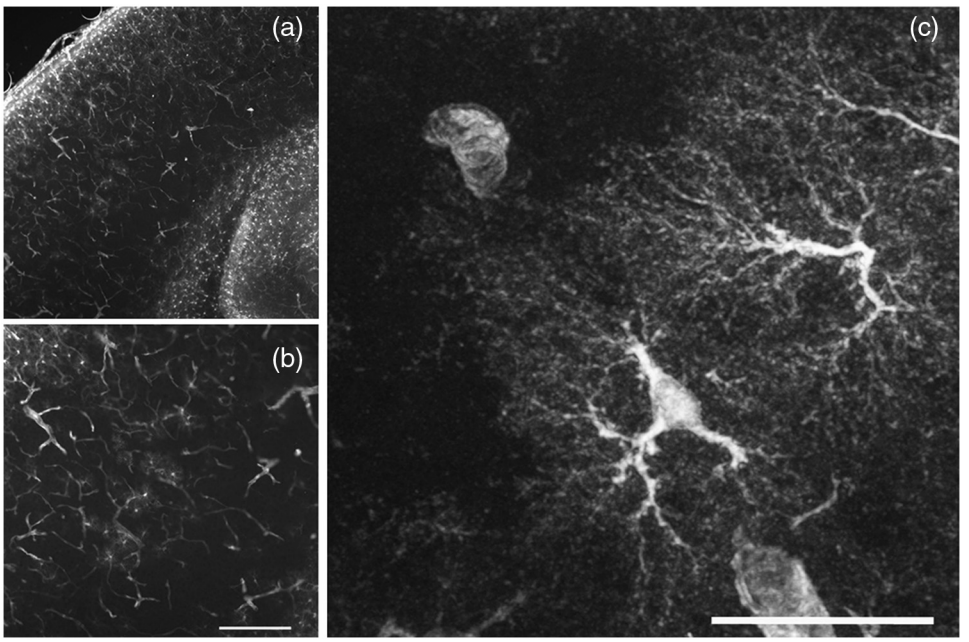

Fig. 1 Expression of EGFP in astrocytes and blood vessels of BAC Id3 mice. Images taken at different magnification showing labeling in astrocytes and blood vessels in somatosensory cortex in fixed brain slices of BAC Id3 mice. Notice the labeling of even small processes in the arbor of astrocytes shown in c. Scale bar = 100 μm (a; 10×, b; 20×; epifluorescence), 25 μm (c; 100×; confocal).

In the cortex, only a fraction of all astrocytes were labeled—cortical layers 1 and 4 contained high densities of labeled astrocytes, while layers 2–4 contained sparse labeling which was largely limited to a subset of vessel-associated astrocytes. The dense labeling of astrocytes in layers 1 and 4 made it difficult to distinguish individual process arbors in many of the labeled astrocytes. However, individual astrocytes were visible in cortical layers 1–3 at all ages, especially at P7. By P61, more deep layer (V-VI) astrocytes were brightly labeled and labeling in superficial layers was less intense, suggesting that deeper layer astrocytes may not be accessible for imaging in this strain at younger ages. The expression profiles were very similar

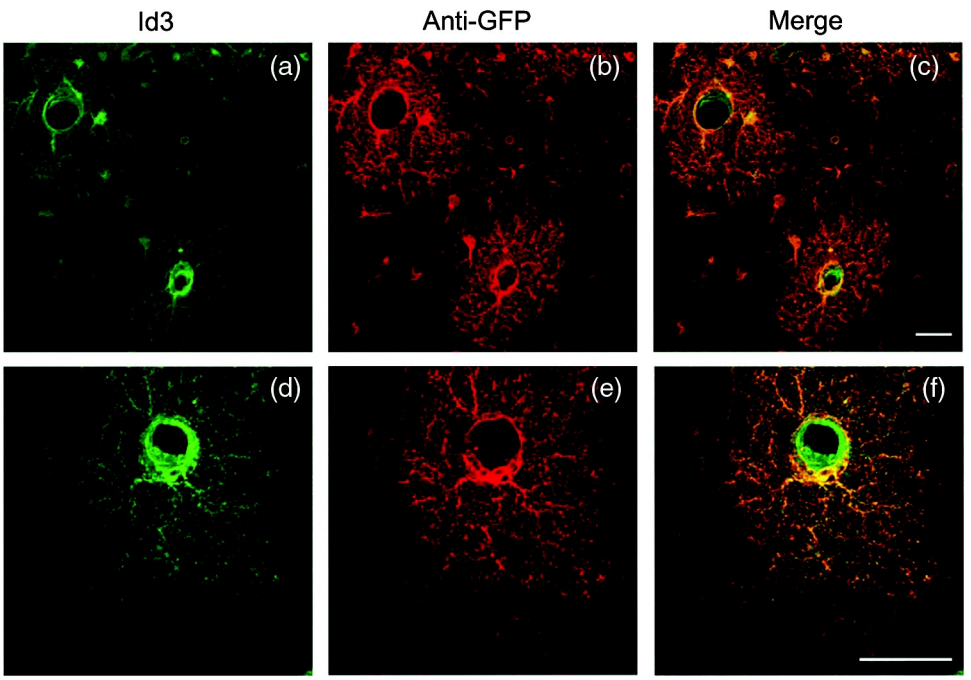

Fig. 2 EGFP expression is high and can be visualized without immunological amplification. Confocal images of EGFP-labeled astrocytes in fixed section of a P61 animal. Astrocytic processes labeled with EGFP (a,d) and also visualized using an anti-GFP antibody (b, e) are shown. Notice that while merged images (c, f) show co-localization of GFP fluorescence and antibody labeling, immunostaining allows a slightly crisper visualization of small processes. Scale bar = 25 μm.

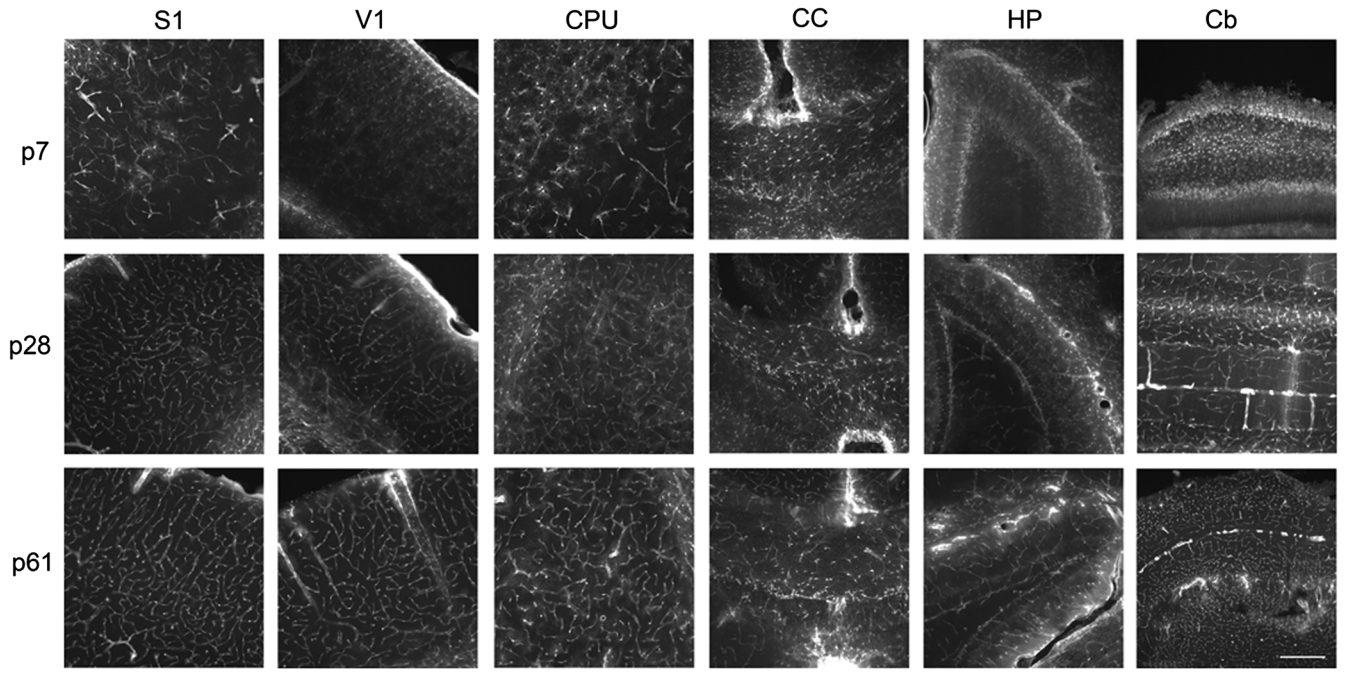

Fig. 3 Developmental expression of EGFP in different brain areas of the BAC Id3 mouse. EGFP epifluorescent images taken in fixed brain sections of animals of different ages in different brain areas at 20× magnification. Most brain areas show similar EGFP expression profiles: staining is intense and astrocytic at earlier ages but most prominent in blood vessels in adult animals. Abbrev: S1 – primary somatosensory cortex, V1 – primary visual cortex, CPU – caudate/putamen; CC – corpus callosum, HP – hippocampus; Cb – cerebellum. Scale bar = 100 μm.

Table 1 Developmental expression of EGFP in different brain areas of the BAC Id3 mouse. A blinded observer categorized EGFP fluorescence in astrocytes and blood vessels in different brain areas at different ages. +, ++, +++ refer to increasing intensity or density of structures (as labeled in the table). A blank means no labeling was observed. N – nets of astrocytes were observed in close proximity to one another. S – single isolated astrocytes were distinguishable. Abbreviations: S1 – primary somatosensory cortex, V1 – primary visual cortex, CC – corpus callosum, CPU – caudate/putamen; HPC – hippocampus; DGc – dentate gyrus granular layer; DGm – dentate gyrus molecular layer; CA1m – CA1 stratum moleculare; CA1r – CA1 stratum radiatum; CA1 – CA1 stratum pyramidale; Cb – cerebellum.

			SI			VI					HPC					
			Layer 1	Layer II/III	Deep Layer	Layer 1	Layer II/III	Deep Layer	cc	CPU	DGg	DGm	CAlm	CAlr	CA1	Cb
P7	Astrocytes	Intensity	+++	++	+	+++	++	+	++	++	+++	+++	+++	++	+	+++
		Density	+++	++	+	+++	++	+	+++	+++	++	+++	+++	+	+	++
		Processes	N	N	N	N	N	N	S	N	S	N	N	N	N	S
	Blood vessels	Intensity	++	++	++	++	++	++	++	++	++	++	++	+	+	
P28	Astrocytes	Intensity	+++	++	+++	+++	++	++	++	++	+	++	+++	+	++	
		Density	++	+	+++	++	+	++	+++	++	+	++	+++	+	++	
		Processes	N	N	N	N	N	N	S	N	S	N	N	N	S/N	
	Blood vessels	Intensity	++	++	++	++	++	++	++	++	+	++	++	+	++	++
P60	Astrocytes	Intensity	++	++	+++	+++	++	+++	+++	++	+	++	+++	+	++	
		Density	++	+	+++	++	+	+++	++	++	+	++	+++	+	++	
		Processes	N	N	N	N	N	S/N	S	N	S	N	N	N	S	
	Blood vessels	Intensity	++	++	+++	++	++	++	+	++	+	++	+++	+	+	++

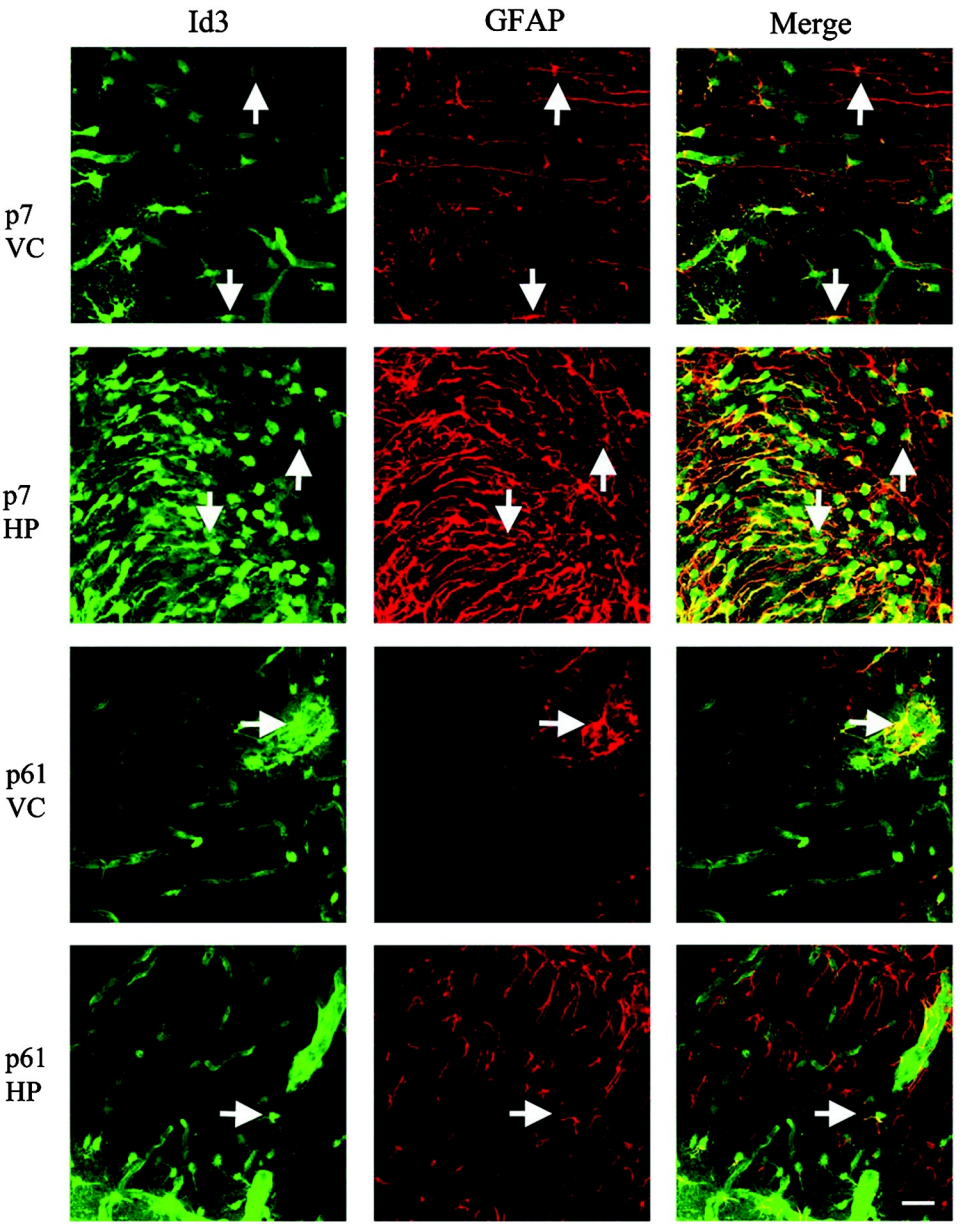

Fig. 4 Co-localization of EGFP with GFAP. Id3 tissue co-labeled with anti-GFAP antibody at P7 (top panels) and P61 (bottom panels) in the visual cortex (VC) and hippocampus (HPC). Many EGFP-labeled cells co-localized with GFAP immunoreactivity (see arrows for examples). Scale bar = 25 μm (40×; confocal microscopy).

across all cortical areas [see comparison of somatosensory cortex (S1) and visual cortex (V1) in Table 1 and Fig. 3]. Labeling of cells in the CA1 area of the hippocampus and in the dentate gyrus was also sparse and layer-specific. White matter regions throughout the brain had large densities of labeled astrocytes. In the corpus collosum, the extent of expression was similar in young and adult animals. Individual astrocytes could be clearly visualized and showed typical morphologies of white matter astrocytes. The profile of labeling in the cerebellum underwent the biggest change with age, with very few blood vessels but with intense astrocytic labeling at P7. By P61, cerebellar blood vessels were intensely labeled and astrocytic labeling was limited to the white matter.

We confirmed the astrocytic nature of the EGFP-labeled elements structurally identified as astrocytes using immunocytochemistry against specific markers of astrocytes, neurons, and microglia. EGFP-labeled cells often co-localized with GFAP immunoreactivity in developing adult animals (Fig. 4). Occasionally, EGFP-labeled cells did not show GFAP immunoreactivity, likely due to the heterogeneous expression of this marker within the astrocytic population. No co-localization of EGFP and immunocytochemical labeling of microglia [Iba-1; Fig. 5(a)] or neurons [NeuN; Fig. 5(b)] were observed.

To determine how well astrocytes could be visualized *in vivo*, we used two-photon microscopy to image cortical astrocytes through an acute cranial window or through a thinned skull window in adult BAC Id3 EGFP mice (Fig. 6). At these ages, fluorescence in superficial layer astrocytes is at its lowest in our developmental timeline, therefore, we were curious as to

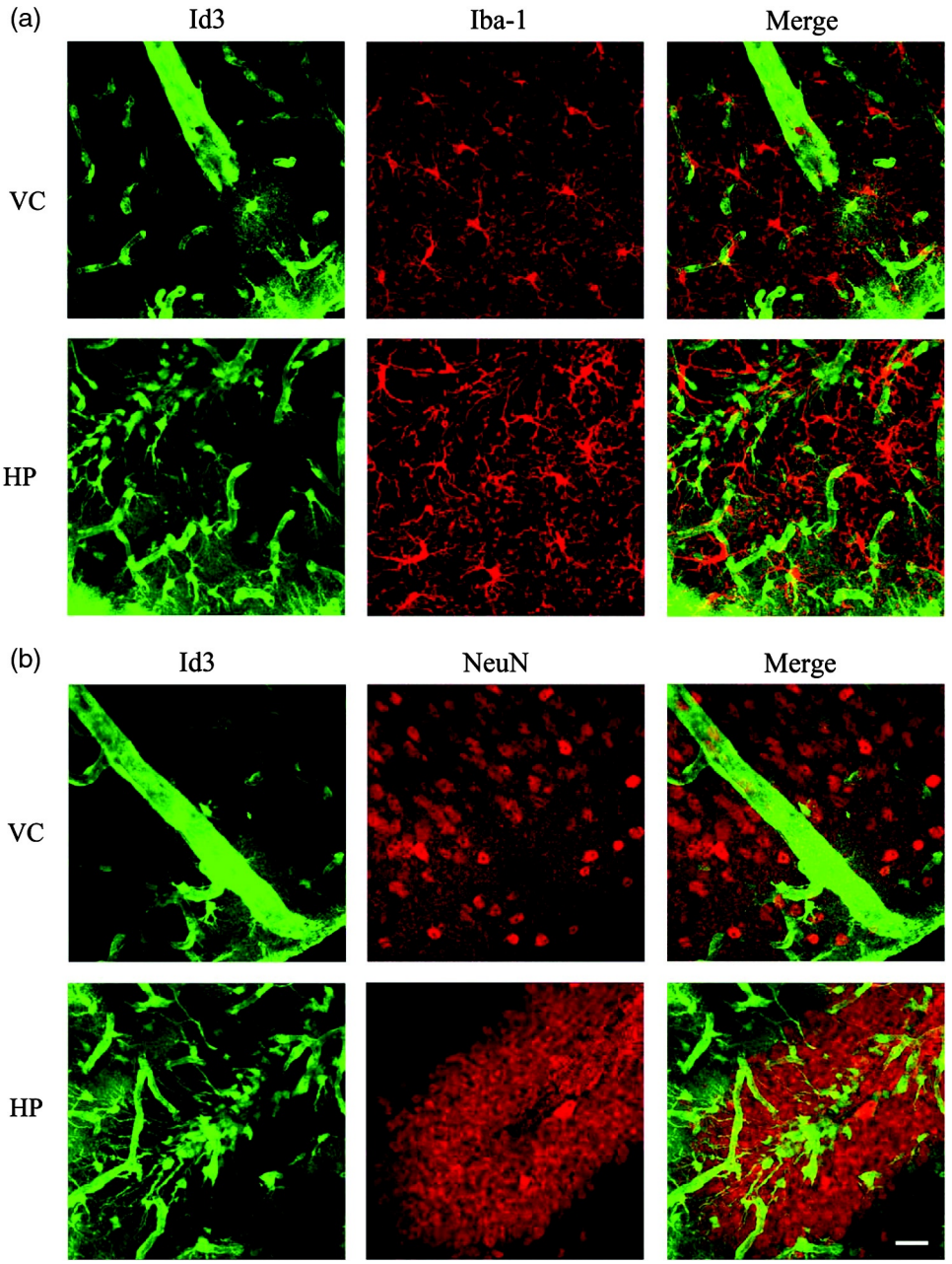

Fig. 5 Lack of co-localization of EGFP with markers of neurons and microglia. P61 Id3 tissue co-labeled with anti-Iba-1 antibody (a) and anti-NeuN antibody (b). EGFP did not co-localize with anti-Iba-1or anti-NeuN staining in the visual cortex (VC) or hippocampus (HP). Scale bar = 25 μm (40×; confocal microscopy).

whether adult astrocytes could be examined *in vivo* using this model. We also reasoned that this would represent the "worst case scenario" for *in vivo* imaging, and if we found that adult astrocytes were visible it would suggest that imaging would also be possible at younger ages. Our *in vivo* imaging recapitulated the expression profiles observed in fixed sections. We noted that blood vessels were easily visualized throughout the depth of our imaging stack (~500 μm below the level of the pia). Astrocytes in layer 1 were also easily visible, but due to the high density of labeled cell bodies, it was difficult to make out individual process morphologies. Within layer 2, individual labeled astrocytes were clearly visible (Fig. 6), and fine processes of the astrocytic process arbor could be delineated at higher magnifications (Fig. 7). To determine whether fine astrocytic processes are motile *in vivo*, as has been described in brain slices,[15–17] we took time-lapse images and tracked fine processes every 5 min over a period of 30 min (Fig. 8). We did not observe any overt changes in the process arbor during this time, suggesting that astrocytic processes in anesthetized animals *in vivo* may be structurally stable on these timescales.[18]

To compare BAC Id3 EGFP mice to other available astrocytic reporter strains, we also carried out *in vivo* imaging experiments on BAC GLT-1 transgenic mice, in which the majority of astrocytes throughout the brain express EGFP.[21] While astrocytes have previously been visualized in these mice using

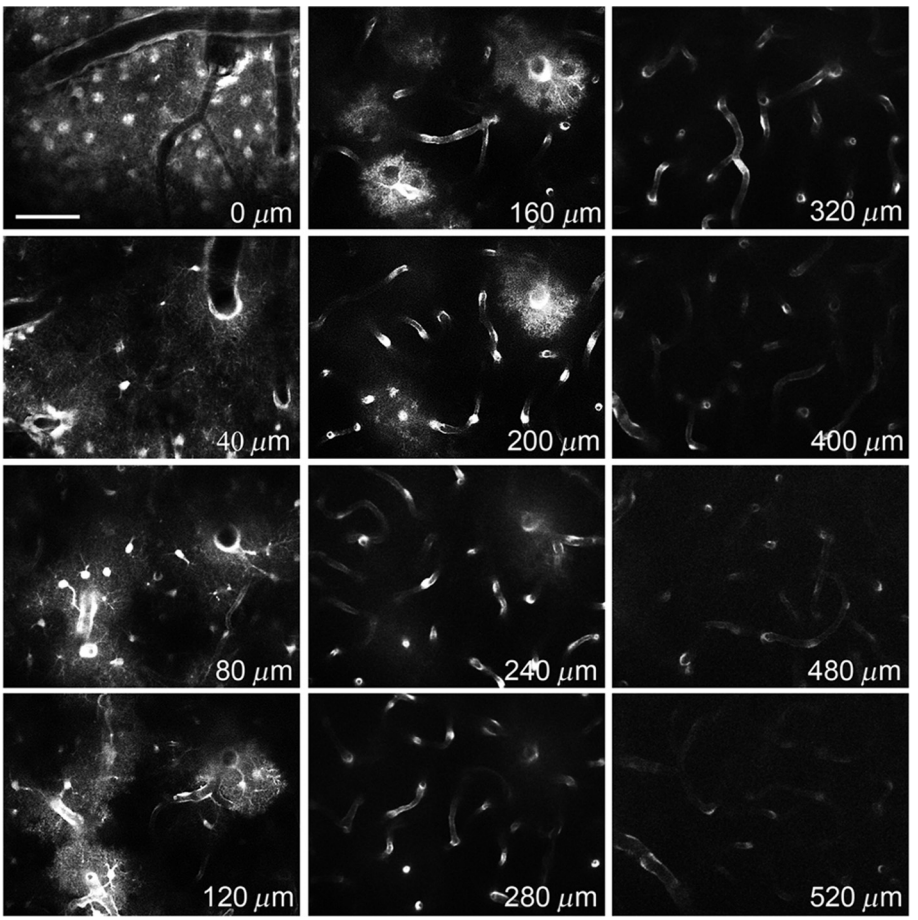

Fig. 6 Visualization of blood vessels and astrocytes in the cortex of BAC Id3 mice *in vivo*. *In vivo* two-photon imaging of EGFP through an acute cranial window in an adult mouse. Images were taken at increasing depth from the level of the pia in the visual cortex (each displayed image is a maximum intensity projection of four images taken at 5-μm intervals). Notice that bright astrocytes are present at the surface while blood vessels are labeled deeper within the brain in agreement with the fluorescent profile observed in our fixed tissue sections. Scale bar = 50 μm.

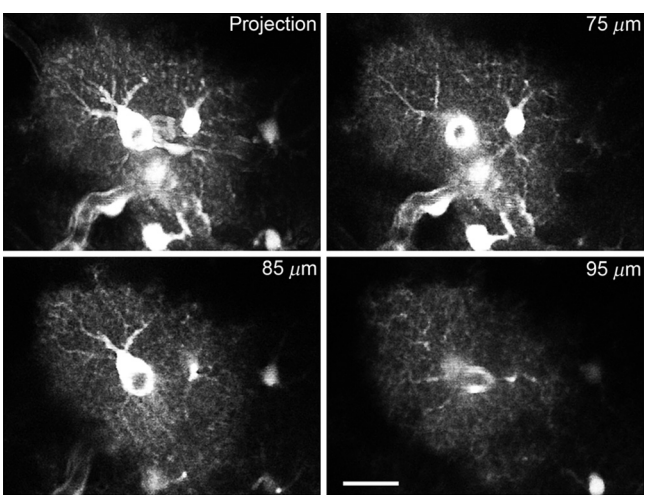

Fig. 7 Visualization of fine astrocytic processes in the cortex of BAC Id3 mice *in vivo*. Astrocytic morphology imaged *in vivo* at higher magnification (10× digital zoom). Images were taken approximately 100-μm below the level of the pia-depth is indicated in the top right corner of each image. Notice that fine astrocytic process morphology is apparent in single optical sections but is obscured somewhat in the maximum intensity projection (top left panel) due to the complexity of the astrocytic arbor. Scale bar = 10 μm.

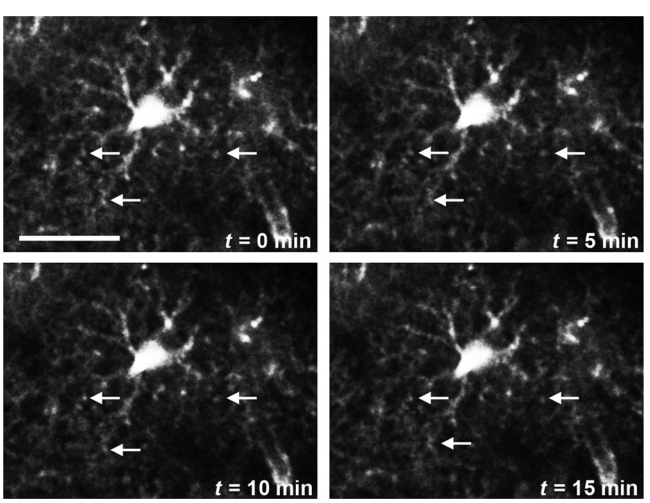

Fig. 8 Astrocytic processes are structurally stable in anesthetized mice. EGFP-labeled astrocytic arbor imaged *in vivo*. A single *z*-plane was imaged over time to examine astrocytic process motility. Images were acquired every 5 min. We observed little change in astrocytic process morphology over time (notice the persistence of structures indicated with arrows throughout the time course shown). Scale bar = 25 μm.

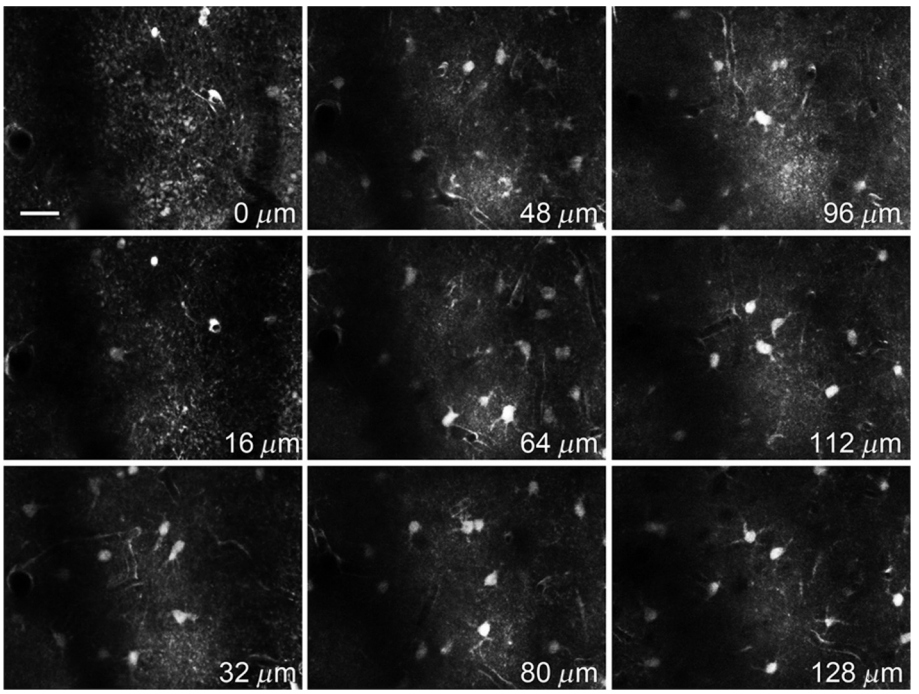

Fig. 9 Visualization of astrocytes in the cortex of BAC GLT-1 EGFP mice *in vivo*. *In vivo* two-photon imaging of visual cortex in an adult BAC GLT-1 EGFP mouse. Images were taken at increasing depth from the level of the pia in the visual cortex (each displayed image is a maximum intensity projection of four images taken at 4-μm intervals). Notice that evenly distributed astrocytic cell bodies and endfeet are visible throughout the imaging area. Fine process structure, however, is not clearly visible except at very superficial depths. Dark bands present in all images are shadows of superficial vasculature. Scale bar = 25 μm.

fixed tissue, their suitability for *in vivo* imaging has not been explored. We found that astrocytes could be visualized *in vivo* in the visual cortex throughout layers 1–3, but that the fine structure of the astrocytic process arbor was not as clearly delineated as in the BAC Id3 EGFP mice, possibly due to the dense labeling of many astrocytes with GFP compared to the sparse labeling in the BAC Id3 EGFP mice (Fig. 9).

4 Discussion

Here, we characterize a transgenic mouse line that potentially allows the *in vivo* imaging of fine astrocytic processes over the course of postnatal brain development. EGFP expression is present in blood vessels and a small population of astrocytes throughout the entire brain of this mouse line. During early development, EGFP expression is more prominent in astrocytes, while in adult animals astrocytes are slightly less extensively labeled and blood vessel labeling predominates. However, even in adult mice, astrocytic fine processes can be visualized in the cerebral cortex *in vivo* using two-photon microscopy. An advantage of this mouse line is that astrocytic labeling is sparse, making it possible to discriminate individual cells as required to study how they interact with blood vessels and neurons. We also show that, at least in adult anesthetized animals, fine astrocytic processes appear structurally stable on short time scales.

4.1 *Id3 Expression in the Postnatal Brain*

Although our main goal was to characterize this mouse line for the *in vivo* imaging of astrocytes, our results also give us insight into the postnatal expression of Id3. Id3 has known roles in early gestational development, where it is critical for promoting angiogenesis and neurogenesis.[19] Much less is known about its function in the postnatal brain, although it has been implicated in tumor growth,[19] immune cell differentiation,[25] wound healing,[26] inflammation,[27] and blood vessel repair.[28] Our findings imply that Id3 expression is developmentally regulated in a cell-type specific manner within different brain regions postnatally, and is restricted to astrocytes and blood vessel wall associated cells. This suggests that Id3 has important roles in the brain vasculature throughout life and is important in the regulation of gene expression in a small number of postnatal astrocytes. In these studies, we focused our attention on astrocytes, therefore, we cannot definitely say which cells in the vascular walls express Id3, although the sparse pattern of astrocyte labeling makes it unlikely that Id3 labeling of the vasculature results from its expression in astrocytic endfeet. Id3 has been shown to be expressed in endothelial cells during development and in tumor vasculature, although its expression is thought to be limited in the adult brain. It is important to note that we could not verify our pattern of Id3 expression in wild-type mice due to the lack of specific tools to track the endogenous Id3 protein. This characterization will be important in future studies of Id3 expression in postnatal animals.

4.2 *Imaging Astrocytes and Blood Vessels in the Intact Brain*

Whether the BAC transgenic mouse faithfully follows the endogenous Id3 expression pattern is less relevant for our main goal of characterizing EGFP expression in astrocytes in these mice. Our results show that EGFP is expressed throughout early postnatal development and adulthood and labels a small

proportion of the astrocytic population. This is reminiscent of the thy-1 XFP mice,[29] which are very popular for *in vivo* imaging studies of neuronal architecture. The sparse labeling of astrocytes allows for easier imaging of fine processes—in fact such structure is lost in areas where many astrocytes are labeled such as in layer 1 of the cerebral cortex in BAC Id3 EGFP mice (Fig. 5), and in GLT-1 mice in which the majority of astrocytes express EGFP (Fig. 9). It is unclear what governs astrocytic expression of EGFP in the BAC Id3 EGFP mouse line. This labeling could be stochastic—where each astrocyte may or may not express EGFP relatively randomly, or labeling may delineate a specific subclass or a small number of subclasses of astrocytes. If the latter is true, this mouse line may allow the imaging of a new class of astrocytes defined by Id3 expression. In fact, most immunohistological markers of astrocytes label only a small fraction of brain astrocytes suggesting that specific functional subtypes, defined by their expression patterns, may exist in the brain. Unfortunately, astrocyte heterogeneity is still a very poorly understood topic,[30] making it all the more important to define and explore different classes of astrocytic cells.

There are many tools for labeling astrocytes *in vivo* because of the importance of studying these cells in their native milieu. Of the organic dyes, sulforhodamine 101 (SR101)[31] has proven to be the most reliable for identifying astrocyte, although its application often requires the opening of the skull and is, therefore, generally only useful for acute experiments (see Refs. 32 and 33). It has been used extensively and can label astrocytic processes.[33] In the majority of studies, however, labeling is largely limited to the soma. SR101 use is further limited by its uptake being age-dependent and brain-region specific,[34,35] and SR101 has also been shown to interfere with plastic processes.[36] Astrocytes have also been labeled using several virus labeling strategies,[15,16,37,38] although studies of astrocytic processes in viral labeled astrocytes have been limited to *ex vivo* preparations.[15,16] The downside of the virus labeling approach is that injection of the virus into the brain can cause damage and inflammation which may alter the course of the experiment. Other transgenic approaches are also available. Most common are the GFAP-EGFP mice, which label only those astrocytes with the highest GFAP expression.[39,40] These mice have been used to image astrocytic fine process dynamics in slice cultures in the cerebellum[41] and astrocytic responses to injury *in vivo*.[12,13] The Aldh1l1-EGFP and mice label the entire astrocyte population.[13,20,42] In these mice, individual processes are not apparent either due to the dense labeling or to the intensity of EGFP expression. Similarly, in our study, the BAC GLT-1 EGFP mouse[21] allowed the visualization of a large population of astrocytes in the superficial layers of visual cortex *in vivo* without providing a clear image of individual fine processes (Fig. 9). In contrast, an astrocytic line that labels the microtubule cytoskeleton has been used to obtain beautiful images of astrocytic processes *in vivo*,[18] however, this line may miss the structure and dynamics of areas supported by other cytoskeletal proteins. Recently, GLAST^{CreERT2} knock-in mice[43] crossed with an inducible reporter line have been used to image astrocytes *in vivo*.[13] A subset of astrocytes, including the astrocytic process arbor, was clearly visible, but the authors did not attempt to image fine morphology. Such a conditional approach could be adapted to the many astrocytic driver Cre mice available and may prove very useful for *in vivo* imaging of fine astrocytic processes in the future.

4.3 *Dynamics of Astrocytic Processes*

Astrocytes interact with synaptic structures and can modulate synaptic transmission and plasticity. Because the coverage of synapses by astrocytic processes is sensitive both to physiological and pathological stimuli,[44,45] it has been proposed that astrocytic processes can be highly dynamic. In organotypic slice cultures, virally labeled astrocytic processes were shown to be more highly motile (on the order of minutes) than their postsynaptic partners.[16] Such dynamic synaptic interactions could serve to stabilize specific synapses within a circuit.[15,17] While the activity-dependent motility of glial processes has been demonstrated *in vivo* in developing brains of unanesthetized xenopus tadpoles,[46] to date there is little evidence to support the high motility of fine astrocytic processes in adults *in vivo*, especially in mammalian systems. This is in part due to the dearth of labeling tools that allow for the visualization of the very small tips of astrocytic processes within the intact brain. The Id3 BAC transgenic mouse allowed us to image the dynamics of fine processes of adult astrocytes *in vivo*. We did not observe any motility of fine astrocytic processes on the timescale of tens of minutes, suggesting that astrocytes in the adult intact brain of anesthetized animals may not be motile. This agrees with *in vivo* imaging of microtubule structures in astrocytic processes, which was also described to be stable on these timescales,[18] and with our time-lapse studies of the dynamics of very superficial fine processes in the BAC GLT-1 EGFP mouse. While we cannot rule out that processes that fall under our detection limit may be motile, it is interesting to note that we could visualize processes that were $\sim 1\ \mu$m in size, similar to the size of motile processes in previous *in vitro* studies of developing systems.[16] In contrast, it is likely that adult astrocytic processes are motile on a slower scale, as observed in response to injury.[13] Such slow motility of astrocytic processes could also be mediated by water fluxes in astrocytes, as astrocytes have been shown to swell in both physiological and pathological conditions,[12,47] regulating extracellular space and intercellular signaling. Recently, the swelling of astrocytes has been shown to be regulated by the sleep wake cycle, allowing the clearance of brain metabolites during sleep.[47] Such subtle changes in astrocytes between different physiological states may regulate astrocytic actions at synapses in the adult more than rapid motility of processes. On the other hand, astrocytic process motility may be differentially regulated in awake and anesthetized animals as has been shown for other astrocytic functions.[9,48] More investigation of the dynamics of astrocytic process arbors *in vivo* in awake animals, both during development and adulthood, using new labeling strategies such as the Id3 BAC transgenic mouse, will be needed to fully understand the role of rapid motility of astrocytes under physiological conditions.

Acknowledgments

We are grateful to Emily A. Kelly and Nina Lutz for technical assistance and Grayson Sipe for comments on the manuscript. We also thank Maiken Nedergaard and Jeffrey Rothstein for generously providing us with the GLT-1 eGFP BAC transgenic mice. This work was supported by a grant from the National Institutes of Health (No. EY019277) to AKM. MET was funded by Fonds de la recherche en santé du Québec (FRSQ) and Canadian Institutes of Health Research (CIHR) postdoctoral training awards. The funders had no role in study design, data collection and analysis, decision to publish, or preparation of the manuscript. Author contributions: A.K.M. designed

research; C.E.L., M-E.T., and A.K.M. performed research; C.E.L. and A.K.M. analyzed data and wrote the manuscript.

References

1. H. K. Kimelberg and M. Nedergaard, "Functions of astrocytes and their potential as therapeutic targets," *Neurotherapeutics* **7**(4), 338–353 (2010).
2. M. Zonta et al., "Neuron-to-astrocyte signaling is central to the dynamic control of brain microcirculation," *Nat. Neurosci.* **6**(1), 43–50 (2003).
3. C. Iadecola and M. Nedergaard, "Glial regulation of the cerebral microvasculature," *Nat. Neurosci.* **10**(11), 1369–1376 (2007).
4. G. Dallerac, O. Chever, and N. Rouach, "How do astrocytes shape synaptic transmission? Insights from electrophysiology," *Front Cell Neurosci.* **7**, 159 (2013).
5. C. Eroglu and B. A. Barres, "Regulation of synaptic connectivity by glia," *Nature* **468**(7321), 223–231 (2010).
6. W. S. Chung et al., "Astrocytes mediate synapse elimination through MEGF10 and MERTK pathways," *Nature* **504**(7480), 394–400 (2013).
7. T. Fellin, "Communication between neurons and astrocytes: relevance to the modulation of synaptic and network activity," *J. Neurochem.* **108**(3), 533–544 (2009).
8. H. Hirase et al., "Calcium dynamics of cortical astrocytic networks in vivo," *PLoS Biol.* **2**(4), E96 (2004).
9. J. Schummers, H. Yu, and M. Sur, "Tuned responses of astrocytes and their influence on hemodynamic signals in the visual cortex," *Science* **320**(5883), 1638–1643 (2008).
10. D. A. Dombeck et al., "Imaging large-scale neural activity with cellular resolution in awake, mobile mice," *Neuron* **56**(1), 43–57 (2007).
11. X. Wang et al., "Astrocytic Ca2+ signaling evoked by sensory stimulation in vivo," *Nat. Neurosci.* **9**(6), 816–823 (2006).
12. J. Sword et al., "Evolution of neuronal and astroglial disruption in the peri-contusional cortex of mice revealed by in vivo two-photon imaging," *Brain* **136**(5), 1446–1461 (2013).
13. S. Bardehle et al., "Live imaging of astrocyte responses to acute injury reveals selective juxtavascular proliferation," *Nat. Neurosci.* **16**(5), 580–586 (2013).
14. M. Nedergaard, J. J. Rodriguez, and A. Verkhratsky, "Glial calcium and diseases of the nervous system," *Cell Calcium* **47**(2), 140–149 (2010).
15. H. Nishida and S. Okabe, "Direct astrocytic contacts regulate local maturation of dendritic spines," *J. Neurosci.* **27**(2), 331–340 (2007).
16. M. Haber, L. Zhou, and K. K. Murai, "Cooperative astrocyte and dendritic spine dynamics at hippocampal excitatory synapses," *J. Neurosci.* **26**(35), 8881–8891 (2006).
17. J. Hirrlinger, S. Hulsmann, and F. Kirchhoff, "Astroglial processes show spontaneous motility at active synaptic terminals in situ," *Eur. J. Neurosci.* **20**(8), 2235–2239 (2004).
18. T. Y. Eom et al., "Direct visualization of microtubules using a genetic tool to analyse radial progenitor-astrocyte continuum in brain," *Nat. Commun.* **2**, 446 (2011).
19. D. Lyden et al., "Id1 and Id3 are required for neurogenesis, angiogenesis and vascularization of tumour xenografts," *Nature* **401**(6754), 670–677 (1999).
20. N. Heintz, "Gene expression nervous system atlas (GENSAT)," *Nat. Neurosci.* **7**(5), 483 (2004).
21. M. R. Regan et al., "Variations in promoter activity reveal a differential expression and physiology of glutamate transporters by glia in the developing and mature CNS," *J. Neurosci.* **27**(25), 6607–6619 (2007).
22. K. B. J. Franklin and G. Paxinos, *The Mouse Brain in Stereotaxic Coordinates*, Academic Press, Waltham, Massachusetts (2008).
23. E. A. Kelly and A. K. Majewska, "Chronic imaging of mouse visual cortex using a thinned-skull preparation," *J. Vis. Exp.* (44), 2060 (2010).
24. A. Majewska, G. Yiu, and R. Yuste, "A custom-made two-photon microscope and deconvolution system," *Pflugers Arch* **441**(2–3), 398–408 (2000).
25. R. R. Rivera et al., "Thymocyte selection is regulated by the helix-loop-helix inhibitor protein, Id3," *Immunity* **12**(1), 17–26 (2000).
26. I. M. Moya et al., "Stalk cell phenotype depends on integration of Notch and Smad1/5 signaling cascades," *Dev. Cell* **22**(3), 501–514 (2012).
27. S. F. Tzeng et al., "Tumor necrosis factor-alpha regulation of the Id gene family in astrocytes and microglia during CNS inflammatory injury," *Glia* **26**(2), 139–152 (1999).
28. D. Lee et al., "Id proteins regulate capillary repair and perivascular cell proliferation following ischemia-reperfusion injury," *PLoS One* **9**(2), e88417 (2014).
29. G. Feng et al., "Imaging neuronal subsets in transgenic mice expressing multiple spectral variants of GFP," *Neuron* **28**(1), 41–51 (2000).
30. Y. Zhang and B. A. Barres, "Astrocyte heterogeneity: an underappreciated topic in neurobiology," *Curr. Opin. Neurobiol.* **20**(5), 588–594 (2010).
31. A. Nimmerjahn et al., "Sulforhodamine 101 as a specific marker of astroglia in the neocortex in vivo," *Nat. Methods* **1**(1), 31–37 (2004).
32. F. Appaix et al., "Specific in vivo staining of astrocytes in the whole brain after intravenous injection of sulforhodamine dyes," *PLoS One* **7**(4), e35169 (2012).
33. A. Perez-Alvarez, A. Araque, and E. D. Martin, "Confocal microscopy for astrocyte in vivo imaging: Recycle and reuse in microscopy," *Front Cell Neurosci.* **7**, 51 (2013).
34. K. W. Kafitz et al., "Developmental profile and properties of sulforhodamine 101–Labeled glial cells in acute brain slices of rat hippocampus," *J. Neurosci. Methods* **169**(1), 84–92 (2008).
35. C. Y. Schnell, Y. Hagos, and S. Hulsmann, "Active sulforhodamine 101 uptake into hippocampal astrocytes," *PLoS One* **7**(11), e49398 (2012).
36. J. Kang et al., "Sulforhodamine 101 induces long-term potentiation of intrinsic excitability and synaptic efficacy in hippocampal CA1 pyramidal neurons," *Neuroscience* **169**(4), 1601–1609 (2010).
37. R. L. Lowery et al., "Rapid, long-term labeling of cells in the developing and adult rodent visual cortex using double-stranded adeno-associated viral vectors," *Dev. Neurobiol.* **69**(10), 674–688 (2009).
38. A. Colin et al., "Engineered lentiviral vector targeting astrocytes in vivo," *Glia* **57**(6), 667–679 (2009).
39. C. Nolte et al., "GFAP promoter-controlled EGFP-expressing transgenic mice: a tool to visualize astrocytes and astrogliosis in living brain tissue," *Glia* **33**(1), 72–86 (2001).
40. L. Zhuo et al., "Live astrocytes visualized by green fluorescent protein in transgenic mice," *Dev. Biol.* **187**(1), 36–42 (1997).
41. T. Lordkipanidze and A. Dunaevsky, "Purkinje cell dendrites grow in alignment with Bergmann glia," *Glia* **51**(3), 229–234 (2005).
42. Y. Yang et al., "Molecular comparison of GLT1+ and ALDH1L1+ astrocytes in vivo in astroglial reporter mice," *Glia* **59**(2), 200–207 (2011).
43. T. Mori et al., "Inducible gene deletion in astroglia and radial glia–a valuable tool for functional and lineage analysis," *Glia* **54**(1), 21–34 (2006).
44. C. Genoud et al., "Plasticity of astrocytic coverage and glutamate transporter expression in adult mouse cortex," *PLoS Biol.* **4**(11), e343 (2006).
45. M. Iino et al., "Glia-synapse interaction through Ca2+-permeable AMPA receptors in Bergmann glia," *Science* **292**(5518), 926–929 (2001).
46. M. Tremblay et al., "Regulation of radial glial motility by visual experience," *J. Neurosci.* **29**(45), 14066–14076 (2009).
47. L. Xie et al., "Sleep drives metabolite clearance from the adult brain," *Science* **342**(6156), 373–377 (2013).
48. A. S. Thrane et al., "General anesthesia selectively disrupts astrocyte calcium signaling in the awake mouse cortex," *Proc. Natl. Acad. Sci. U. S. A.* **109**(46), 18974–18979 (2012).

Cassandra Lamantia is a technical associate in the laboratory of Ania Majewska in the Department of Neurobiology and Anatomy at the University of Rochester Medical Center.

Marie-Eve Tremblay is an assistant professor at Laval University, Quebec City, Canada. Her lab is investigating the roles of immune cells in the experience-dependent remodeling of neuronal circuits in different contexts of health and disease, using a combination of noninvasive imaging techniques.

Ania Majewska is an associate professor in the Department of Neurobiology and Anatomy at the University of Rochester Medical Center. Her lab investigates the mechanisms of activity-dependent plasticity.